

Self-Shielding Copper Substrate Neutron Supermirror Guides

P. M. Bentley^{1,5}, R. Hall-Wilton^{1,3,4}, C. P. Cooper-Jensen¹, N. Cherkashyna¹, K. Kanaki¹, C. Schanzer², M. Schneider², P. Böni²

E-mail: phil.m.bentley@gmail.com, richard.hall-wilton@ess.eu, base548@kateandcarsten.com, Nataliia.Cherkashyna@ess.eu, kalliopi.kanaki@ess.eu, christian.schanzer@swissneutronics.ch, michael.schneider@swissneutronics.ch, peter.boeni@frm2.tum.de

¹ European Spallation Source ERIC, Box 176, 221 00 Lund, Sweden

² Swiss Neutronics AG Neutron Optical Components & Instruments, Brühlstrasse 28, CH-5313 Klingnau, Switzerland

³ Università degli Studi di Milano-Bicocca, Piazza della Scienza 3, 20126 Milano, Italy

⁴ University of Glasgow, Glasgow, United Kingdom

⁵ Anderson Butovich Ltd. United Kingdom

Abstract. The invention of self-shielding copper substrate neutron guides is described, along with the rationale behind the development, and the realisation of commercial supply. The relative advantages with respect to existing technologies are quantified. These include ease of manufacture, long lifetime, increased thermal conductivity, and enhanced fast neutron attenuation in the keV-MeV energy range. Whilst the activation of copper is initially higher than for other material options, for the full energy spectrum, many of the isotopes are short-lived, so that for realistic maintenance access times the radiation dose to workers is expected to be lower than steel and in the lowest zoning category for radiation safety outside the spallation target monolith. There is no impact on neutron reflectivity performance relative to established alternatives, and the manufacturing cost is similar to other polished metal substrates.

Keywords: Neutron optics, metal substrate, copper substrate, supermirror, neutron shielding

1. Introduction

With the imminent delivery of the first copper substrate neutron guides to the European Spallation Source (ESS), currently under construction in Sweden, it is timely to briefly

report on the rationale for, and development of, this new technology, and compare it to established alternatives.

Neutron guides are solid tubes, usually of rectangular cross section. The optimisation of the geometry of these devices is a very broad topic and out of the scope of this paper. Here it is sufficient to note that instrument angular resolution, transport efficiency and background rejection often — but not always — tend to favour a channel width in the region of 4-6 cm, and due to mechanical stability requirements the substrates themselves are typically around 1 cm thick.

On the internal surfaces, neutron mirrors are deposited to maximise the transmission of neutrons to the experimental stations. This allows the placement of the instrument remotely from the neutron source, some 10s or even 100s of metres away, reducing instrumental background and facilitating safe physical access designs. Historically, single, smooth metallic layers were used as neutron mirrors, but modern neutron guides use alternating Ni-Ti layers known as “supermirrors” [1].

In a typical neutron source, one has a means of neutron production (fission, fusion, or spallation) and a volume of temperature-controlled, strongly-scattering material known as a moderator. The optical interface between the neutron guides and the region within a few metres of the moderator is often known as the “beam extraction” area, and specific technology exists to improve the instrument performance. The neutron optics work in the beam extraction area carries greater technical challenges due to:

- The energy produced along with neutrons creating a large heat load
- A high radiation environment
- A need for good reflective properties at large angles near the source

High albedo, rad-hard materials are used around the moderator (e.g. beryllium, with some recent interest in nanodiamond, particularly for cold wavelengths [2]) where the grazing angles are large. At distances typically 1-2 metres from the moderator, the grazing angles are below the critical angles on supermirrors, but that still leaves heat- and radiation-loads that must be carefully managed.

For the neutron guides entering the beam extraction area, polished metal [3] and glass-ceramic [4] optics have existed for some time and offer a robust, long-lifetime solution for high radiation environments. Indeed, irradiation tests indicate that supermirrors on metallic substrates do not show any degradation to a cumulative neutron fluence of $9 \times 10^{19} \text{ n cm}^{-2}$ [5]. This is comparable to sodium float glass ($\sim 1 \times 10^{20} \text{ n cm}^{-2}$), and orders of magnitude higher than boron-containing glass substrates ($\sim 1 \times 10^{18} \text{ n cm}^{-2}$ for some borokron variants and $\sim 1 \times 10^{16} \text{ n cm}^{-2}$ for borofloat). These fluences are integrated over the entire source spectrum, based on studies at the reactor source of the Institut Laue-Langevin (ILL, Grenoble, France) and the spallation source of the Paul Scherrer Institut (PSI, Villigen, Switzerland).

They are assembled from shapes very similar to the glass guide variants, but instead of bonding by adhesives they are bolted together. In addition to improved lifetime, they also have the potential to enhance the fast neutron and gamma ray shielding

properties of the guide system, by increasing the density of the material immediately outside the supermirror channel. With the preceding technology, there is always a gap of several centimetres between the supermirror surface and the bulk shielding material, to allow for glass substrates, adjustment, and vacuum housings. The new idea here is to bring dense shielding material into direct contact with the supermirror. This can correspondingly reduce the total volume of shielding needed downstream through geometrical considerations, by placing the most effective shielding in the key locations where it will have the greatest impact.

It is important to note that the shielding effect is in the longitudinal direction by virtue of the long line integral for low divergence beams, and thus the advantages are in the far-field sense. The transverse shielding effect is minimal, since the guide substrates themselves are only ~ 1 cm thick and perhaps 2 metres of heavy shielding is required in the beam extraction area; indeed locally there should be an enhanced gamma production from neutron capture.

Further benefits of metal substrates over glass are improved thermal conductivity, structural properties and robustness, which could allow the guides to be placed close to the neutron source without thermal damage occurring. Of particular interest is using these for guide inserts for in-monolith beam extraction from the target-moderator region at spallation sources. However, regions further out where fast neutrons are present may benefit from strategically placed effective shielding as well.

Inspiration for the use of copper as a shielding material for fast neutrons at spallation sources came in part from experience of its use at other accelerator facilities and in high energy physics experiments. The possibility for its application here is motivated by the same advantages: its shielding effect for fast neutrons, thermal conductivity and structural properties. A couple of examples are given below:

In the Large Hadron Collider [6] the area with the most intense radiation environment is around the experimental interaction points where the two beams collide. To protect the delicate superconducting accelerator equipment from such intense radiation and thermal loads, there are two key protective elements: the TAS and the TAN. The Tertiary Absorber of Secondaries (TAS) is a 1.8m long block of copper weighing around 2 tonnes and located at ~ 20 m from the interaction point, which blocks high energy particles from exiting the experimental cavern into the LHC tunnel; and the Tertiary Absorber of Neutrals (TAN) [7], which is a 3.5m long copper block, designed to absorb neutral particles (neutrons and pions) at about 140m from the interaction point, which can have energies up to the beam energy (7 TeV).

The hadronic calorimeter of the CMS instrument is made from brass [8], whose stopping power for high energy particles compares favourably with the steel calorimeter on ATLAS [9]. Unpublished concepts from JPARC were also influential, where Cu had been used in the collimation of instruments for the same reasons [10].

This manuscript looks at using copper for the multifunctional purpose as substrate to the neutron supermirror guide, thermal transport and radiation shielding. Cost prevents deploying copper shielding liberally, but in some targeted areas it would be

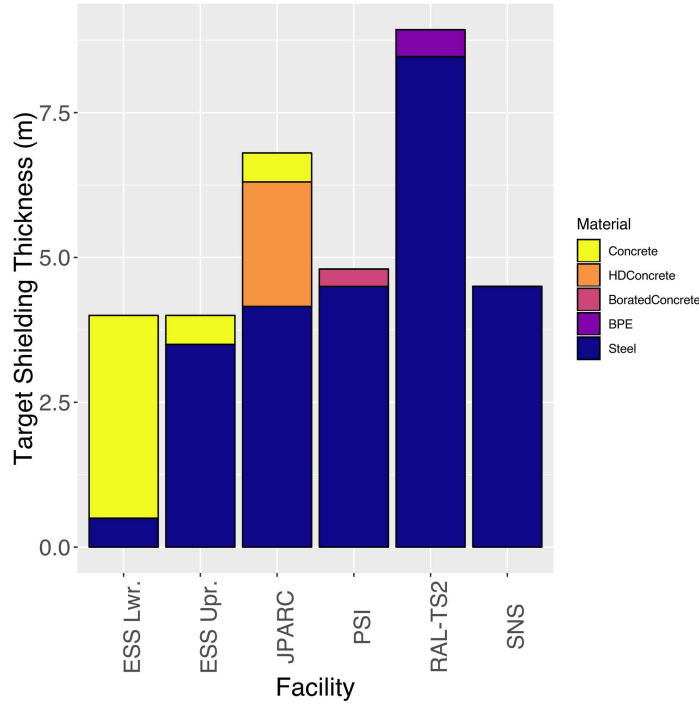


Figure 1. Comparison of different spallation target shielding concepts at various leading facilities around the world, both operational and under construction. The ESS has two concepts, a lower part and an upper part. A design change reduced the steel shielding for the lower parts physically below the neutron beam port level to save money.

ideal.

2. Shielding at Spallation Sources

The initial motivation for the copper guides, and copper shielding in general, was to reduce fast neutron background signals on the instruments of the ESS, based on investigations of challenges faced by similar, operational facilities [11]. Shielding is a significant fraction of a neutron facilities cost, both in terms of shielding the source and shielding the instruments. Indeed, shielding and optics together represent half of the total cost of constructing an instrument at a spallation source [12].

Attempting to build the most powerful neutron spallation source in the world, with the least amount of target shielding in the world, is a challenging proposition from a background perspective. Figures 1 and 2 give some insight into the raw numbers of this challenge, and it should be no surprise that Target Station 2 (TS2) at the Rutherford Appleton Laboratory (RAL), in Oxford (UK) hosts the instruments with world-leading signal to noise ratios (e.g. [13]). This gives motivation to the quest for better shielding.

The ESS Neutron Optics and Shielding group was formed to learn from these other facilities and propose technical strategies related to optics and shielding for the parts of the facility that are external to the target system [12, 14]. Collaboration with the ESS

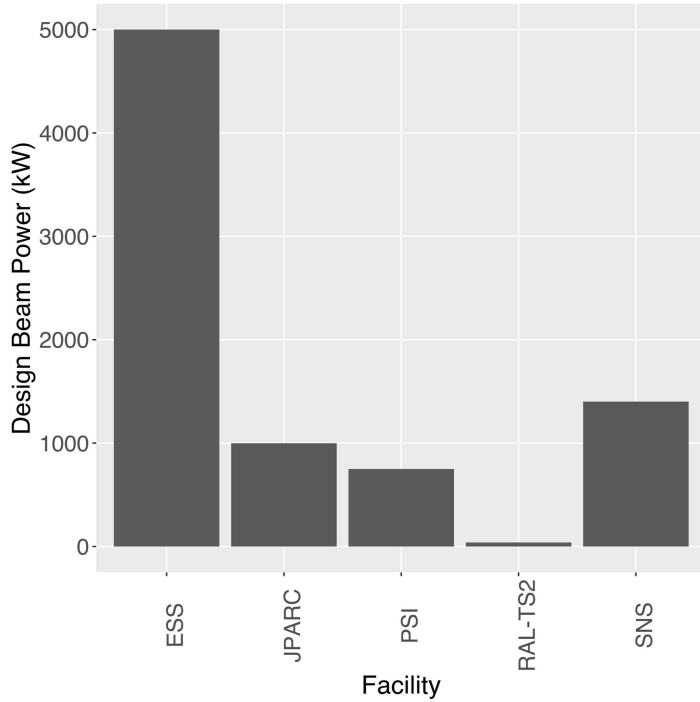


Figure 2. Comparison of different spallation target design powers at various leading facilities around the world, both operational and under construction.

Detector group, who also had an interest in reducing fast neutron backgrounds, brought the team to the realisation that there were potential gains from exploring alternatives to steel shielding in key locations [14]. The need to minimise fast neutron backgrounds is made especially poignant by the relatively high sensitivity of thermal neutron detectors, especially ^3He -based detectors, to fast neutrons [15, 16, 17].

It is best practice to shield as close to the radiation source as one can. The primary area of concern is the beam-extraction area, however one also needs to add heavy shielding near penetrations through bulk shielding walls downstream, and regions where one aims to lose direct line of sight to the source by curving the guides. In these areas we had the idea to improve the shielding properties of the optical components, so that there was no gap between the supermirror and the shielding material. This means replacing glass and aluminium with heavier elements. In most shielding situations facing a high energy neutron beam, under normal circumstances one would like to use steel as the primary material. Whilst it is possible to polish steel as a substrate for supermirrors, the problem with the iron nucleus — known since the 1980s — is the presence of resonance lines that act as transparent windows, which may be linked to fast neutron background problems [18]. To put this into perspective, the cross section of Fe in parts of this energy range is comparable to that of beryllium for cold neutrons. Cooled Be filters are commonly used neutron optical components [19] to scatter out short wavelength neutrons and transmit cold neutrons, thus one can visualise steel as a filter that scatters thermal neutrons and, to some degree, MeV–GeV neutrons, but transmits readily in the

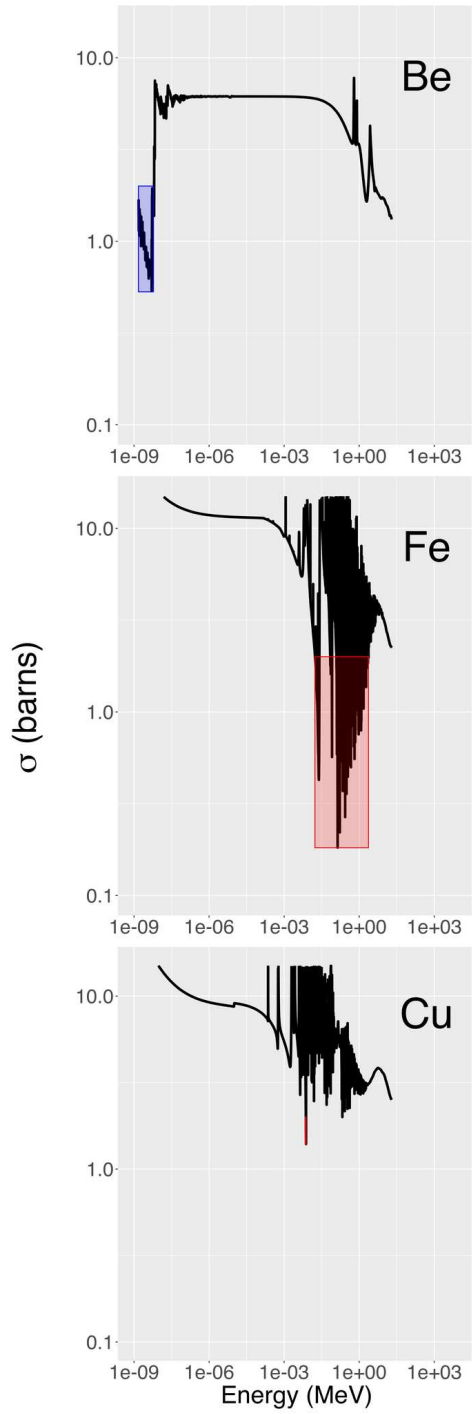


Figure 3. Total neutron cross section of Be, Fe and Cu *vs* energy. The Be data are spliced ENDF [20] and EXFOR [21] data, whilst those for Fe and Cu are ENDF data only. This is because the ENDF data for Be do not contain the transparent region at low energy. The “transparent” region of the Be cross section is shaded with a blue box, with which one should compare the equivalent red box for Fe.

keV–MeV range with only modest attenuation. This is shown in figure 3, highlighting the transparent regions.

There were a lot of myths in the community regarding these resonance windows and fast neutron background effects, which had to be systematically addressed at the outset. For example, some proposed using high-carbon steels as a general shielding material, with the idea that the carbon atoms act as a moderator within the metal and close the transparency windows. “High” carbon steels are $\sim 1\%$ carbon by weight, most steels are fractions of a $\%$ carbon by weight, so this has minimal effect. Another myth was that the background problem could be eliminated by increasing the counting time of the experiment. This confuses systematic error with statistical error. Fast neutron backgrounds vary as a function of time within the data collection window, and furthermore they depend on the configuration of the entire experimental suite and thus vary from measurement to measurement [22], invalidating a simple subtraction. The *raison-d’être* of high power spallation sources is to improve measurements of weak phenomena that are not possible at existing, lower power facilities, and such measurements are disproportionately hindered by systematic and varying background effects that resemble spurious signals. Experience elsewhere suggests that it is difficult to remove these effects and they can impose significant operational limitations on measurements with the instruments.

A final myth, and perhaps the most common, espouses the ignoring of the problem entirely, relying on the idea that the fast neutron background can be discriminated in time. The underlying physics is that of albedo reflections [23] and photonuclear processes ($\gamma \rightarrow n$ reactions) [24] by which fast neutrons are generated, and propagate down curved guides, when no protons are illuminating the spallation target. These two effects combine to create long tailed distributions that exponentially approach a flat asymptote between 10^{-2} and 10^{-4} relative to the prompt $p + W \rightarrow n$ peak, as seen in operational instruments at existing spallation sources [11, 25]. The precise asymptote level depends on the activation of the target, the geometry of the Be, and to what degree the beamline shielding was designed to impede fast neutron transport down the guide system. The characteristic width of the multi-exponential tail depends on the spatial dimensions of the guide channels, the instrument cave, the experimental hall, and the degree to which the shielding designs aim to minimise fast neutron background signals.

In response to these identified risks, in 2013 the ESS teams formulated a mitigation strategy [14]. The definition of this strategy, and the areas in which it was and was not followed, are outside the scope of this article. However, part of the core strategy was to examine the use of superior shielding concepts close to the neutron beamlines.

With steel as a primary shielding material, ideally one would like to attach a second laminate layer, in the form of a hydrogenous material, to deal with these resonant neutrons that shine through the primary shielding. Hydrogenous material is an effective moderator in the energy range of the Fe resonance windows, and boron can be added to conveniently absorb the thermalised neutrons that are emitted downstream. The boron capture gamma is just under 0.5 MeV which makes it excellent in regards to subsequent photonuclear production. For this reason, borated polyethylene (BPE) and borated paraffin wax feature heavily downstream of the primary steel shielding in the neutronics

design of TS2 at RAL. At the Paul Scherrer Institut, in Villigen (Switzerland), water tanks are used that are filled with dilute boric acid.

Concrete is often used as a cheap alternative to borated hydrogenous materials, with much compromised performance. The water content and density of concrete are rather low, so the cost savings are not proportional. For this reason, a separate project studied concrete hydration [26] and developed a modified recipe for this purpose [27, 28]. This is fine for instrument shielding and external shielding surfaces along beamlines, but is not intended for shielding within a radius of a few 10s of cm from the neutron beamlines close to the source target to reduce fast neutron contributions.

In the case of the ESS it was established that polymer solutions are unsuitable for this use case, with a lifetime of only a few months when the facility reaches its MW power classification [29]. This is because, as a long pulse source, ESS may have a time-averaged neutron source brightness comparable to the most powerful reactor source in the world — the Institut Laue-Langevin (ILL) in Grenoble, France — significantly exceeding anything offered by short pulse spallation sources. For this reason, copper is an attractive material that may offer comparable shielding characteristics to a steel laminate solution, without the short lifetime of polymers. There is only one significant resonance line creating a transparency in copper. In early models of simple bulk materials, copper provided more than an order of magnitude suppression relative to iron for fast neutrons [18]. Bags of copper shot in the gap between the neutron guide and the shielding have subsequently been used to achieve a 25% reduction in the prompt pulse background [11] on the CNCS Instrument at SNS (ORNL), Oak Ridge, US.

3. Method

Being an item that is covered by nuclear licensing documentation, it is important to specify the materials used in the preparation of the substrate. The coppers documented for use are CW008A and more recently CW021A. The substrate was cut, chamfered, polished and cleaned according to the usual procedure at Swiss Neutronics AG. Whilst copper is more expensive than aluminium as a raw material, the preparation of copper is only slightly more challenging than other materials. Furthermore, the main cost drivers are subsequent to the substrate preparation stages, so that there is a negligible economic difference between the metal substrate options. This simplifies the derivation of a technical strategy for instrumentation [12], since only one metal substrate cost needs to be considered, and the detailed design can specify the substrate at a later stage.

The substrates were loaded onto the deposition facility in the normal way, and an $m = 3$ Ni-Ti supermirror was deposited according to the standard commercial recipe used in other $m = 3$ optical components. Peel tests were passed, indicating good mirror adhesion equivalent to other substrate materials. Waviness measurements indicated no adverse effects relative to other substrates, and the dimensional parameters all lie within the usual engineering tolerances as are typical for other materials.

After fabrication, the supermirror samples were taken to the ILL and the reflectivity

curve measured on the D17 neutron reflectometer [30], and the Narziss neutron reflectometer at PSI, to validate the quality of the mirrors.

Meanwhile, the shielding performance and activation of the materials were assessed using Geant4 [31, 32, 33] and PHITS v3.17 / DCHAIN [34] respectively, relative to other materials. The fast neutron attenuation between both these packages was verified to be in agreement. In a separately published study, as part of the development programme, the shielding properties were compared between Geant4 and neutron measurements at 174.1 MeV and found to be in excellent agreement [35].

The activation calculations assumed a worker maintenance scenario. Another unique design decision in the ESS was to remove heavy shutters in the target monolith, as a cost saving measure. Such beam shutters are used regularly at existing neutron sources to turn off individual beams for maintenance work without disturbing the operations of other instruments outside of the work area. The lack of such shutters means that maintenance work at ESS will only be possible in the beam extraction area during a complete shutdown of the facility, allowing some additional time for removing the shielding. It also means that all of the technical staff will experience the same intensive burst of activity every shutdown, with a strong motivation to access equipment as early as possible in order to maximise the amount of repair during the shutdown window. Nonetheless, the unstacking of the shielding bunker requires considerable effort and at least one day — probably longer.

The calculations assumed an irradiation time of 5000 days, with the ESS running at 5 MW proton beam power, using the least divergent, 0.1° , cone of a source term generated from detailed spallation target models that was later published as an internal reference standard for the project [36]. This simulated irradiation time is equivalent to 20 years of full power use assuming annual cycles permitting 250 beam days. Nine separate cooldown time points were simulated after proton beam shutdown, these are: 0, 1, 6 hours and 1, 2, 4, 7, 14, 30 days. The simulated starting material is pure copper (CW008A). To give perspective, a range of other common materials were compared that might be found close to the beam port at spallation sources.

The location of the simulated material is outside the target monolith at 6.5 m radius, to establish the activation conditions that maintenance work may encounter with an unshielded guide component, which is why the higher divergence columns can be ignored in the source term. A micro-kernel calculation was used to integrate the total dose rate for a worker, assuming a 1 metre long guide section, 0.07 m tall, and a $0.4 \times 1 \text{ m}^2$ human placed at 0.3 m distance from the material. A more precise estimate may be required for a specific, licensed task, however this estimate allows one to compare materials adequately.

The PHITS/DCHAIN activation calculations were cross-checked against independent MCNP5 [37] simulations of nuclear inventory performed by the spallation target team [38], and no noteworthy differences were found between the two sets of results.

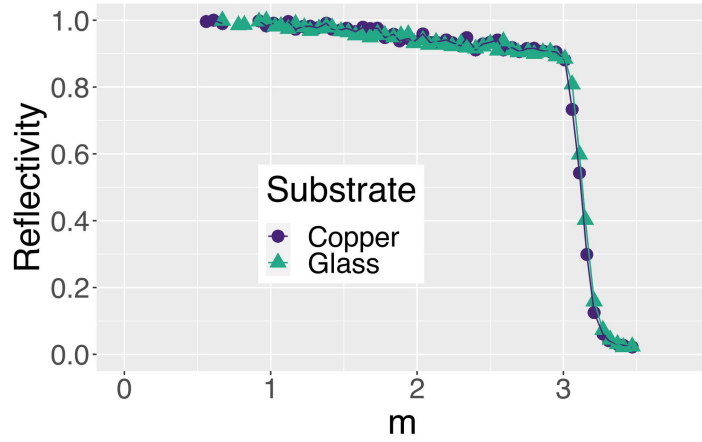


Figure 4. Neutron reflectivity measurements of an $m = 3$ supermirror on a production polished copper metal substrate, performed on the Narziss neutron reflectometer at PSI.

4. Results and Discussions

4.1. Reflectometry

The reflectivity curve for the copper $m = 3$ supermirror in production is shown in figure 4, where $m = 1$ corresponds to the critical angle for total external neutron reflection of smooth nickel ($\approx 0.1^\circ \times \lambda$, where the neutron wavelength λ is given in Å units). There one can see that the neutron optical performance is excellent, and the copper substrate has no effect at all on the supermirror — as expected.

4.2. Simulated Neutronic Properties

The simulated dose rate to a worker, resulting from fast neutron activation, is shown in figure 5. Here one sees that for the first few days, copper is amongst the most active materials, matching instrumentation experience with copper monochromators, for example. However, after ~ 3 days, the copper dose rate drops below that of steel, and after approximately one week copper would be expected to just enter the dose rate for “green” zone classification in Sweden ($< 3 \mu\text{Sv/h}$). 3–7 days of cooldown time for maintenance access to guides close to a neutron source is not unreasonable, based on experience at other facilities. In the same period, mild steel is around $6 \mu\text{Sv/h}$. This is also not problematic *per se* but requires additional assessments, and one should also bear in mind that the equipment inventory is quite dense close to the spallation target

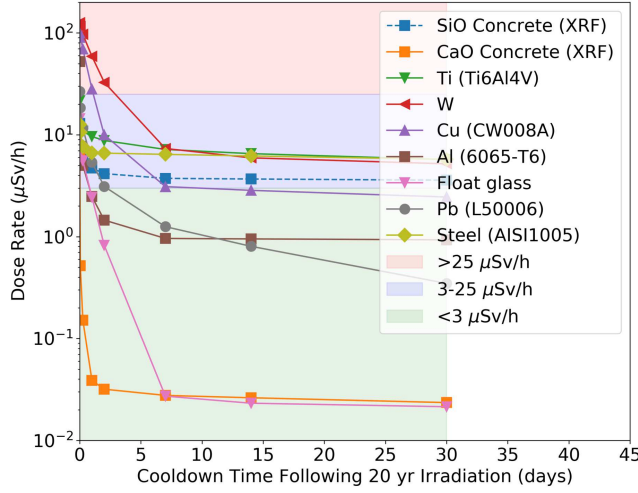


Figure 5. DCHAIN-based micro-kernel estimation of integrated dose rate of a human worker 0.3 m from a $1 \times 0.07 \text{ m}^2$ guide element assuming copper, compared with other materials common to spallation source engineering.

structure, so one is not dealing only with one activated source. For this reason, best practice in nuclear engineering is to use the “ALARA” principle, which stands for “As Low As Reasonably Achievable”. Reducing the dose rate by 50% for no additional cost seems reasonable.

Figure 5 also shows other materials that are interesting from an ESS shielding point of view. Lead is an excellent fast neutron shielding material, with an expected dose rate at all times lower than copper and steel, and even below aluminium after ~ 12 days. As lead is also a good gamma attenuator, it makes sense to line the front face of heavy shielding walls close to the source with lead to both reduce the fast neutron activation downstream and its resulting gamma shine, both improving the dose rate for workers.

One can also see the benefit of replacing silicate aggregates with limestone aggregates in concrete — the input material composition of both these concrete curves was generated from x-ray fluorescence (XRF) measurements of concrete samples from a local supplier. This matches the experience in Japan of Suzuki *et al* [39], for example.

The primary isotopes for medium-term management of fast-neutron activated copper are summarised in table 1. The three main isotopes contribute almost equally. One expects ^{58}Co with a half life of 2 months, and ^{60}Co with a half-life of around 5.3 years, and ^{54}Mn with a half life of 10 months.

These isotopes are generated in copper at a much lower rate than in other shielding materials, even though they are similar to well known nuclear waste problems. For example, in steel, ^{54}Mn is produced by relatively common — 70 millibarns (mb) — $^{54}\text{Fe}(n,p)^{54}\text{Mn}$ fast neutron reactions and this accounts for the overwhelming majority ($>70\%$) of the worker dose in the first months after shutdown. The copper channel is less than 1/4 of that, at 16 mb, and comes from cascade processes.

Table 1. Table of most significant gamma contributors in copper, after 20 years of fast neutron activation 6.5 metres from the ESS target monolith followed by 30 days cooldown, determined using PHITS v3.17 and DCHAIN.

Isotope	Dose Contribution (%)	Half Life
^{58}Co	31.5	2 mo
^{60}Co	27.0	5.3 yr
^{54}Mn	19.2	10 mo
^{48}V	8.4	16 d
^{56}Co	6.0	77 d

Some stainless steels are known for rapidly accumulating dangerous levels of ^{60}Co , but this is from *thermal* neutron absorption in ^{59}Co with a cross section of 37 barns, where cobalt is typically a few % by weight as a nickel impurity. This process vastly exceeds the copper production rate simulated here, with a *fast neutron* cross section of 14 mb, via the $^{63}\text{Cu}(n,\alpha)^{60}\text{Co}$ reaction. Finally, ^{58}Co production occurs, again via high energy cascades, at 28 mb. For an overview of these higher energy isotope cross sections see the following references [40, 41, 42, 43].

Reactor scientists who have worked with copper, as a monochromator on a diffraction instrument for example, are used to the high levels of activation in the first days. Thermal neutron activation of copper produces ^{64}Cu , a beta emitter with a half life of just under 13 hours, decaying to ^{64}Ni and ^{64}Zn which are both stable. The second thermal activation isotope is ^{66}Cu , decaying to ^{66}Zn with a half life of just over 5 minutes, which is stable. These both dominate in the early stages of cooldown, but the maintenance worker dose from copper is significantly driven by only the spallation products at higher energy, which have longer half lives. It is for these reasons that copper should be expected to allow arms' length maintenance work after a few days of cooldown time, whilst steels fall into the stricter radiation safety categories. Neutron activation should not be an impediment to the use of copper close to high power spallation source beam lines. It has less activity than steels, with superior shielding performance of fast neutrons.

4.3. Gamma Attenuation

It is also worth briefly considering not just the direct fast neutron attenuation but also the gamma attenuation improvements of copper substrate guides, which can reduce downstream photonuclear contributions and shielding load generally. As shown in table 2, the half value layer (HVL) values indicate that copper is slightly better than steel, but more importantly just over a factor of 2 better than aluminium, with gains over glass expected to be similar given the similar densities of glass and aluminium.

Table 2. Gamma attenuation half value layer (HVL) of some example materials, for ^{60}Co Gamma [44].

Material	Density (g cm^{-3})	HVL (mm)
H ₂ O	1.0	108
Al	2.7	46.5
Fe	7.89	16.5
Cu	8.90	14.8
Pb	11.25	10.5

Table 3. Thermal conductivity of some candidate substrate materials [45, 46].

Material	Thermal Conductivity ($\text{W m}^{-1} \text{K}^{-1}$)
Al	235
Fe	80
Cu	400
Glass	~ 1

4.4. Mechanical Factors

The thermal conductivity of copper, compared to other metals, is found in table 3. There one sees that copper offers substantial benefits for cooling possibilities in high power spallation sources. Whilst all of these materials are usable as substrates, the use of copper facilitates the design process to meet the temperature requirements of the monolith guide inserts by nature of its significantly increased thermal conductivity.

4.5. Production and Supply

Copper substrates are now available in full industrial production. The first units are arriving at ESS in Sweden for the VESPA instrument at the time of writing, and the next unit is currently being manufactured — a photograph of one of those mirrors is shown in figure 6, which also shows bolt-holes for assembly and grooves for multi-channel optical wafers. High m -value mirrors up to $m = 6$ have been produced.

All of the ESS instruments requiring supermirrors within the target monolith are using copper substrates, at the time of writing there are 7 units at varying stages of procurement. Several instruments are also planning to order copper substrates in the near future, for some of the key locations described earlier and in previous documentation [14] along with copper shielding blocks.

5. Conclusions

Supermirrors with polished copper substrates have been developed and are now available via routine commercial supply, at a similar cost to other metal substrates. They have



Figure 6. Photograph of a supermirror deposited on a copper substrate, in preparation for assembly. Also visible are bolt-holes for assembly and, to the right, grooves for inserting multi-channel optical wafers.

been shown to offer excellent optical performance, on par with any other substrate. There are no production issues expected to impact on longevity.

As part of an integrated concept of improved Cu-based shielding close to high power spallation neutron beamlines, the combined developments are expected to deliver significantly improved fast neutron attenuation. However, the ultimate background performance also depends on holistic design across the facility, which is beyond the scope of this article.

The main drawback is an enhanced activation level for the first 3 days, compared to steel for example. However, taking into account *realistic* maintenance access planning, this should not be an issue. Indeed, for long shutdowns — the kind where significant access would be expected in the beam extraction area around spallation targets — after a cooldown of ~ 7 days, the copper substrates themselves with 20 years of irradiation at the ESS could allow maintenance work in the easiest safety category according to Swedish legislation. The actual access will most likely depend on whether there are more active items nearby. This is superior to all steels under the same conditions.

Finally, copper offers a superior thermal conductivity compared to other substrates,

which facilitates the design of either active or passive cooling systems with which to protect the supermirrors themselves against thermal degradation.

6. Acknowledgements

S. Ansell, D. D. DiJulio and V. Santoro are gratefully acknowledged for interesting scientific discussions that helped us with some of the ideas in this work and other closely related papers.

7. References

- [1] F. Mezei. Novel polarized neutron devices: supermirror and spin component amplifier. *Communications on Physics (London)*, 1(3):81–85, 1976.
- [2] V. Nesvizhevsky, U. Köster, M. Dubois, N. Batisse, L. Frezet, A. Bosak, L. Gines, and O. Williams. Fluorinated nanodiamonds as unique neutron reflector. *Carbon*, 130:799–805, 2018.
- [3] C. Schanzer, P. Böni, and M. Schneider. High performance supermirrors on metallic substrates. *Journal of Physics: Conference Series*, 251:012082, 2010.
- [4] C. Lartigue, J. R. D. Copley, F. Mezei, and T. Springer. Focusing of neutron beams using curved mirrors for small angle scattering. *Journal of Neutron Research*, 5(1):71–79, 1996.
- [5] C. Schanzer, M. Schneider, and P. Böni. Metallic substrates for advanced applications in neutron optics. In *Design and Engineering of Neutron Instruments (DENIM) Conference*, 2016.
- [6] Lyndon Evans and Philip Bryant (ed). LHC machine. *Journal of Instrumentation*, 3:S08001, 2008.
- [7] LHCf Collaboration. The LHCf detector at the CERN large hadron collider. *Journal of Instrumentation*, 3:S08006, 2008.
- [8] G. L. Bayatian et al. CMS the hadron calorimeter technical design report. Technical report, CERN-LHCC-97-031 CMS-TDR-2, 1997.
- [9] A. Succurro. The ATLAS tile hadronic calorimeter performance in the LHC collision era. *Physics Procedia*, 37:229–237, 2012.
- [10] M. Arai. Private communication, 2015.
- [11] N. Cherkashyna, R. J. Hall-Wilton, D. D. DiJulio, A. Khaplanov, D. Pfeiffer, J. Scherzinger, C. P. Cooper-Jensen, K. G. Fissum, S. Ansell, E. B. Iverson, G. Ehlers, F. X. Gallmeier, T. Panzner, E. Rantsiou, K. Kanaki, U. Filges, T. Kittelmann, M. Extegarai, V. Santoro, O. Kirstein, and P. M. Bentley. Overcoming high energy backgrounds at pulsed spallation sources. *Proceedings of the 21st Meeting of the International Collaboration on Advanced Neutron Sources (ICANS-XXI)*, 2014.
- [12] P. M. Bentley. Instrument suite cost optimisation in a science megaproject. *J. Phys. Commun.*, 4:045014, 2020.
- [13] S.M. Bennington R.I. Bewley, J.W. Taylor. Let, a cold neutron multi-disk chopper spectrometer at isis. *Nuclear Instruments and Methods in Physics A*, 637:128, 2011.
- [14] C. Zendler, V. Santoro, S. Ansell, N. Cherkashyna, D. Martin Rodriguez, C. Cooper-Jensen, D. DiJulio, and P. M. Bentley. European spallation source neutron optics and shielding guidelines, requirements and standards. Technical report, ESS-0039408, 2015.
- [15] F. Piscitelli et al. Verification of He-3 proportional counters’ fast neutron sensitivity through a comparison with He-4 detectors. *Euro Physics Journal Plus*, 135:577, 2020.
- [16] G. Mauri et al. Evidence of fast neutron sensitivity for ^3He detectors and comparison with boron-10 based neutron detectors. *Euro Physics Journal Techniques and Instruments*, 6:3, 2019.
- [17] G. Mauri et al. Fast neutron sensitivity of neutron detectors based on boron-10 converter layers. *Journal of Instrumentation*, 13:P03004, 2018.

- [18] N. Cherkashyna, K. Kanaki, T. Kittelmann, U. Filges, P. Deen, K. Herwig, G. Ehlers, G. Greene, J. Carpenter, R. Connatser, R. Hall-Wilton, and P. M. Bentley. High energy particle background at neutron spallation sources and possible solutions. *Journal of Physics: Conference Series*, 528:012013, 2014.
- [19] D. C. Tennant. Performance of a cooled sapphire and beryllium assembly for filtering of thermal neutrons. *Review of Scientific Instruments*, 59:380, 1988.
- [20] M. B. Chadwick et al. ENDF/B-VII.1 nuclear data for science and technology: Cross sections, covariances, fission product yields and decay data. *Nuclear Data Sheets*, 112:2887–2996, 2011.
- [21] N. Otuka et al. Towards a more complete and accurate experimental nuclear reaction data library (EXFOR): International collaboration between nuclear reaction data centres (NRDC). *Nuclear Data Sheets*, 120:272–276, 2014.
- [22] M. B. R. Smith, E. B. Iverson, F. X. Gallmeier, and B. L. Winn. Mining archived HYSPEC user data to analyze the prompt pulse at the SNS. Technical report, ORNL/TM-2015/238, 2015.
- [23] R. C. Brockhoff and J. K. Shultis. A new approximation for the neutron albedo. *Nuclear Science and Engineering*, 155:1–17, 2007.
- [24] L. Szilard and T. A. Chalmers. Detection of neutrons liberated from beryllium by gamma rays: a new technique for inducing radioactivity. *Nature*, 134:494–495, 1934.
- [25] P. M. Bentley. Early operational challenges for the european spallation source in the sphere of shielding and optics. *In preparation*, 2021.
- [26] L. Wadsö, C. P. Cooper-Jensen, and P. M. Bentley. Assessing hydration disturbances from concrete aggregates with radiation shielding properties by isothermal calorimetry. *Physical Review Accelerators and Beams*, 20:043502, 2017.
- [27] D. D. DiJulio, C. P. Cooper-Jensen, H. Perrey, K. Fissum, E. Rofors, J. Scherzinger, and P. M. Bentley. A polyethylene-B₄C based concrete for enhanced neutron shielding at neutron research facilities. *Nuclear Instruments and Methods in Physics Research A*, 859:41–46, 2017.
- [28] D. D. DiJulio, C. P. Cooper-Jensen, I. Llamas-Jansa, S. Kazi, and P. M. Bentley. Measurements and monte-carlo simulations of the particle self-shielding effect of B₄C grains in neutron shielding concrete. *Radiation Physics and Chemistry*, 147:40–44, 2018.
- [29] N. Tsapatsaris and S. Ansell. Radiation dose and lifetime calculations for sealing materials used at neutron choppers at the ESS. Technical report, European Spallation Source ESS-0084036, 2018.
- [30] R. Cubitt and G. Fragneto. D17: the new reflectometer at the ILL. *Applied Physics A*, 74:s329–s331, 2002.
- [31] S. Agostinelli et al. Geant4 - a simulation toolkit. *Nuclear Instruments and Methods A*, 506:250–303, 2003.
- [32] J. Allison et al. Geant4 developments and applications. *IEEE Transactions on Nuclear Science*, 53:270, 2006.
- [33] J. Allison et al. Recent developments in geant4. *Nuclear Instruments and Methods A*, 835:186, 2016.
- [34] Tatsuhiko Sato, Yosuke Iwamoto, Shintaro Hashimoto, Tatsuhiko Ogawa, Takuya Furuta, Shin ichiro Abe, Takeshi Kai, Pi-En Tsai, Norihiro Matsuda, Hiroshi Iwase, Nobuhiro Shigyo, Lembit Sihver, and Koji Niita. Features of particle and heavy ion transport code system (PHITS) version 3.02. *Journal of Nuclear Science and Technology*, 55(6):684–690, 2018.
- [35] D. D. DiJulio, C. P. Cooper-Jensen, H. Björgvinsdóttir, Z. Kokai, and P. M. Bentley. High-energy in-beam neutron measurements of metal-based shielding for accelerator-driven spallation neutron sources. *Physical Review Accelerators and Beams*, 19:053501, 2016.
- [36] V. Santoro, D. DiJulio, P. M. Bentley, and L. Zanini. Source term for shielding design of bunker and beamlines at ESS. Technical report, ESS-0416080, 2019.
- [37] MCNP. <https://mcnp.lanl.gov/>. Technical report, Los Alamos National Laboratory - LA-UR-03-1987, 2003 (Revised 2008).
- [38] L. Zanini. Shielding of the neutron beam port inserts during extraction: baseline solution.

- Technical report, European Spallation Source ESS-0094274, 2017.
- [39] A. Suzuki, T. Iida, J. Moriizumi, Y. Sakamura, J. Takada, K. Yamasaki, and T. Yoshimoto. Trace elements with large activation cross section in concrete materials in Japan. *Journal of Nuclear Science and Technology*, 38(7):542–550, 2001.
 - [40] J. M. Sisterson and J. Ullmann. Measurements of energy integrated cross sections for reactions producing relatively short-lived radionuclides using neutron beams with an energy range of 0.1–750 MeV. *Nuclear Instruments and Methods in Physics Research B*, 234:419–430, 2005.
 - [41] J. W. Meadows, D. L. Smith, L. R. Greenwood, R. C. Haight, Y. Ikeda, and C. Konno. Measured fast-neutron activation cross sections of Ag, Cu, Eu, Fe, Hf, Ni, Tb and Ti at 10.3 and 14.8 MeV and for the continuum neutron spectrum produced by 7 MeV deuterons on a thick Be-metal target. Technical report, Argonne National Laboratory ANL/CP-74797; CONF-9110261-3, 12 1991.
 - [42] R. Michel, D. Hansmann, S. Neumann, W. Glasser, H. Schuhmacher, V. Dagendorf, R. Nolte, U. Herpers, A. N. Smirnov, I. V. Ryzhov, A. V. Prokofiev, P. Malmberg, D. Kollár, and J.-P. Meulders. Excitation functions for the production of radionuclides by neutron-induced reactions on C, O, Mg, Al, Si, Fe, Co, Ni, Cu, Ag, Te, Pb, and U up to 180 MeV. *Nuclear Instruments and Methods in Physics Research B*, 343:30–43, 2015.
 - [43] A. Van Ginneken and A. Turkevich. Production of manganese 54 and zinc 65 from copper in thick targets by 0.45-Gev, 1.0-Gev, and 3.0-Gev protons. *Journal of Geophysical Research*, 75:5121–5137, 1970.
 - [44] R. Thoraes. Attenuation of gamma radiation from ^{60}Co , ^{137}Cs , ^{192}Ir , and ^{226}Ra in various materials used in radiotherapy. *Acta Radiologica*, 3:81–86, 2009.
 - [45] NIST. NIST standard reference database 81 NIST heat transmission properties of insulating and building materials. <http://dx.doi.org/10.18434/T4RC7M>, 1983.
 - [46] C. Y. Ho, R. W. Powell, and P. E. Liley. Thermal conductivity of the elements. *Journal of Physical and Chemical Reference Data*, 1(2):279, 1972.